Temperature dependent optical properties of ZnO thin film using ellipsometry and photoluminescence

M.-B. Bouzourâa, Y. Battie, S. Dalmasso, M.-A. Zaïbi, M. Oueslati, A. En Naciri

Accepted Manuscript

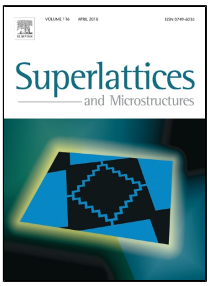

Temperature dependent optical properties of ZnO thin film using ellipsometry and photoluminescence

M.-B. Bouzourâa, Y. Battie, S. Dalmasso, M.-A. Zaïbi, M. Oueslati, A. En Naciri

PII:	S0749-6036(18)30372-0
DOI:	10.1016/j.spmi.2018.03.078
Reference:	YSPMI 5608
To appear in:	*Superlattices and Microstructures*
Received Date:	22 February 2018
Accepted Date:	29 March 2018

Please cite this article as: M.-B. Bouzourâa, Y. Battie, S. Dalmasso, M.-A. Zaïbi, M. Oueslati, A. En Naciri, Temperature dependent optical properties of ZnO thin film using ellipsometry and photoluminescence, *Superlattices and Microstructures* (2018), doi: 10.1016/j.spmi.2018.03.078

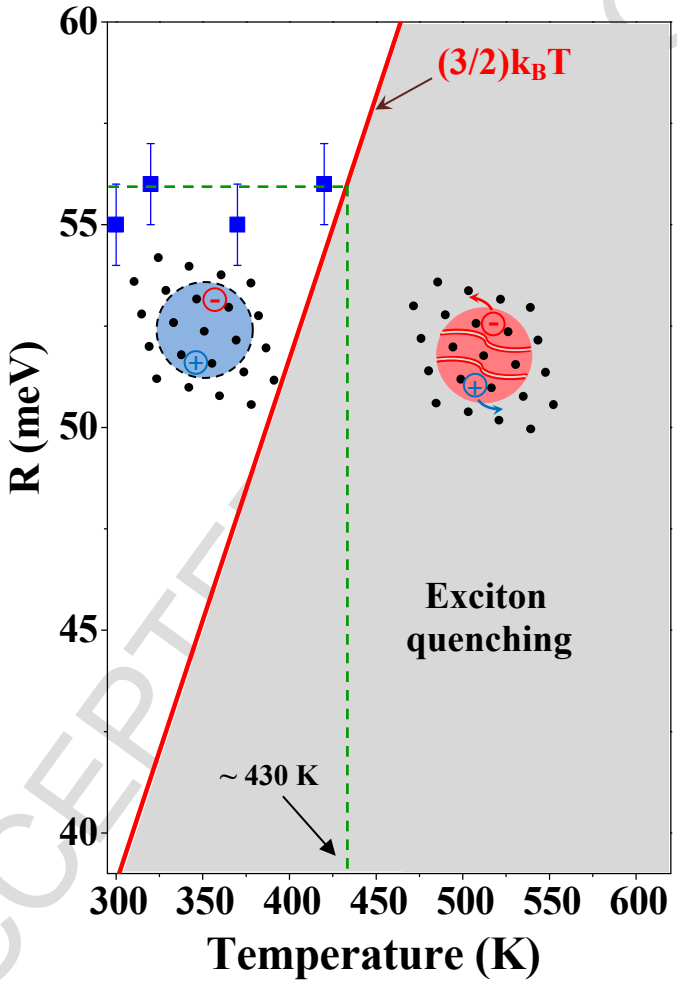

Temperature dependent optical properties of ZnO thin film using ellipsometry and photoluminescence

M.-B. Bouzourâa[1,2*], Y. Battie[1], S. Dalmasso[1], M.-A. Zaïbi[3,4], M. Oueslati[2], A. En Naciri[1*]

[1]LCP-A2MC, Institut Jean Barriol, Metz, Université de Lorraine, France
[2]UNP, Université de Tunis El Manar, Tunis, Tunisia
[3]Université de Tunis, Ecole Nationale Supérieure des Ingénieurs de Tunis, Tunis, Tunisia
[4]Laboratoire LANSER, Centre de Recherche de Borj-Cédria Hammam-Lif Tunis, Tunisia

[*]*Corresponding authors:*

montassar-billeh.bouzouraa@univ-lorraine.fr, Aotmane.en-naciri@univ-lorraine.fr

ABSTRACT

We report the temperature dependence of the dielectric function, the exciton binding energy and the electronic transitions of crystallized ZnO thin film using spectroscopic ellipsometry (SE) and photoluminescence (PL). ZnO layers were prepared by sol-gel method and deposited on crystalline silicon (Si) by spin coating technique. The ZnO optical properties were determined between 300 K and 620 K. Rigorous study of optical responses was achieved in order to demonstrate the quenching exciton of ZnO as a function of temperature. Numerical technique named constrained cubic splines approximation (CCS), Tauc-Lorentz (TL) and Tanguy dispersion models were selected for the ellipsometry data modeling in order to obtain the dielectric function of ZnO. The results reveals that the exciton bound becomes widely flattening at 470 K on the one hand, and on the other that the Tanguy dispersion law is more appropriate for determining the optical responses of ZnO thin film in the temperature range of 300 K to 420 K. The Tauc-Lorentz, for its part, reproduces correctly the ZnO dielectric function in 470 K to 620 K temperature range. The temperature dependence of the electronic transition given by SE and PL shows that the exciton quenching was observed in 420 K to ~520 K temperature range. This quenching effect can be explained by the equilibrium between the Coulomb force of exciton and its kinetic energy in the film. The kinetic energy was found to induce three degrees of freedom of the exciton.

Keywords

ZnO; Ellipsometry; Photoluminescence; Temperature; Dielectric function; Exciton.

1. Introduction

Zinc oxide (ZnO) is a versatile functional semiconductor owing to its interesting characteristics such as: wide band-gap ~3.37 eV, large exciton binding energy ~60 meV at room temperature (RT), transparency, abundance in nature, high electron mobility, thermal stability and piezoelectric properties. These characteristics make ZnO as a promising candidate for several applications in optoelectronics [1, 2], photocatalytic [3], gaz sensing [4], transducers [5] and solar cells [6]. The knowledge of the temperature dependence of the ZnO optical properties is a crucial issue to exploit ZnO devices in harsh conditions.

Spectroscopic ellipsometry (SE) technique is a powerful tool to determine the optical constant of materials [7, 8]. As the ellipsometry is an indirect characterization tool, the combination of a dispersion law and a physical model is required to exploit SE data. Several dispersion laws such as Forouhi-Bloomer [9], Tauc-Lorentz (TL) [10], Tanguy [11] were used to extract the optical constants of ZnO by modeling spectroscopic ellipsometry (SE) data. Recently Gilliot *et al.*[12] have successfully described the ZnO dielectric function at RT using numerical technique based on the constrained cubic spline (CCS) [13]. This technique is consistent with Kramers-Kronig relations [14].

Rai *et al.*[15, 16] have investigated the optical properties of ZnO thin films by transmittance spectroscopy from 78 K to 450 K. They have demonstrated a linear dependence between Urbach energy and the exciton band [15]. The absorption spectrum exhibits a defect bound in the visible spectral range [16]. Due to the presence of exciton band, they have shown that the Tauc plot does not yield to an accurate energy gap value. Therefore, the authors have proposed a physical model, which takes into account the Urbach tail, the exciton transition and the valence band to conduction band transition. However, this model does not reproduce correctly the absorption spectra of ZnO at 300 K [16]. Hauschild *et al.*[17] have reported the temperature dependence of the band-gap energy and the broadening of the exciton luminescence band of ZnO thin films grown by metal-organic vapor phase epitaxy. They have also proposed a physical model to explain the origin of the band-gap shift with increasing temperature. Indeed, the band-gap shift was explained by a combination of the lattice dilatation and the electron-phonon interaction. In these previous works in literature, the temperature dependence of the exciton binding energy have not considered in the analysis of the Urbach energy [15], the absorption spectrum [16] and the band-gap energy shift [17]. In addition, the studies of optical constants by SE have focused on the ZnO optical characteristics at only the RT [18–23].

In the present work, we have determined the ZnO dielectric function by SE in temperature range of the 300 K to 620 K. Firstly, the CCS was selected for the ellipsometry data modeling in order to obtain the dielectric function of ZnO. Then, the obtained dielectric function was fitted by TL and Tanguy dispersion equations. The temperature dependence of the exciton binding energy was determined using both Tanguy and TL models. We observe that the exciton bound becomes widely flattening at 470 K and that the Tanguy dispersion is more appropriate for determining the optical response of ZnO thin films in the temperature range of 300 K to 420 K. However, the Tauc-Lorentz reproduces correctly the ZnO dielectric function in 470 K to 620 K temperature range. The electronic transition energy extracted from the imaginary part of dielectric function was studded by taking into account the exciton quenching. In addition, a rigorous comparison between temperature dependent SE and photoluminescence (PL) measurements is given and analyzed.

2. Experimental

We have used the sol-gel method to elaborate the ZnO thin film. The concentration of ZnO in methoxyethanol was taking 0.6 mol/L. The molar ratio of ZnO to monoethanolamin was maintained to 1. The mixture was, then, stirred for 2 hours at 60°C. Monethanolamin (MEA) is used at the same time as a base and a complexing agent [24]. The resulting solution was kept 48 hours in aging at RT. A droplet of particles in suspension was deposited by spin coating at 3000 rpm on crystalline silicon substrate (Si). A preheating step at 250 °C is used to evaporate the solvents and to remove the organic residues [25]. This deposition and preheating process was repeated eight times. Finally, the films were annealed at 600°C during 2 hours. This annealing temperature has been chosen in order to obtain a good crystal quality necessary to observe the optical exciton effect [1].

The optical response of ZnO layers were investigated using a phase modulated ellipsometer (Horiba Jobin Yvon, UVISEL) in the 0.6 eV–4.6 eV spectral range. The measurements were performed at an angle of incidence of 70° by varying the temperature from 300 K to 620 K with a LINKAM heating system.

Ellipsometry measures the changes of the polarization state between the incident and the reflected light on the samples. The measured values are the ellipsometric angles Ψ and Δ. They are related to the ratio between the reflection coefficients of the sample for p-polarized light (r_p) and s-polarized light (r_s) by the following relationship [8]:

$$r_p / r_s = \tan\psi e^{i\Delta}, \qquad \text{Eq. (1)}$$

The UVISEL ellipsometer measures the I_S and I_C parameters which are related to the ellipsometric angles by [26]:

$$I_s = \sin 2\psi \sin\Delta \quad \text{and} \quad I_c = \sin 2\psi \cos\Delta. \qquad \text{Eq. (2)}$$

Temperature dependent PL measurements were carried out, using a monochromator with a 600 grooves/mm grating combined with CCD camera (spectral resolution of 0.23 nm) over a wide range of temperature from 10 K to 300 K in a He closed-circuit cryostat. For the higher temperature, the measurements were performed using LINKAM heating system from 300 K to 620 K. The excitation was performed at 325 nm (~3.82 eV) by using a feeble power 5 mW He-Cd laser to avoid heating up the sample.

3. Results and discussion

3.1 Spectroscopic ellipsometry measurements

Fig. 1 shows the variation of Ic and Is ellipsometric spectra measured for ZnO deposited on Si substrate. In the spectral range between 0.65 eV and 2 eV (I), Ic and Is show no change with the temperature. In this range, the ZnO is transparent and the observed interferences with large oscillations amplitude can be attributed to the multiple internal reflections at the interface between the ZnO film and Si substrate. In the spectral range from 2.1 eV to 3.5 eV (II), the Ic and Is spectra show that the exciton contribution changes with the temperature. This exciton band, showed in Fig. 1, traduces the crystalline quality of ZnO layer. The X-Ray diffraction of ZnO was performed and that give the same results that reported in our previous work where the ZnO is crystallized in a hexagonal wurtzite lattice with c-axis perpendicular to the substrate [27]. We can see clearly in the insert of Fig. 1 that the exciton behavior is shifted to lower energies and its amplitude decreases with the temperature. Concerning the spectral range between 3.5 eV and 4.6 eV (III), Ic and Is show no variation with the temperature. This energy range is characterized by high absorption resulting from the inter-band transitions in ZnO film. More information can be obtained after modeling Ic and Is spectra by a selected physical model.

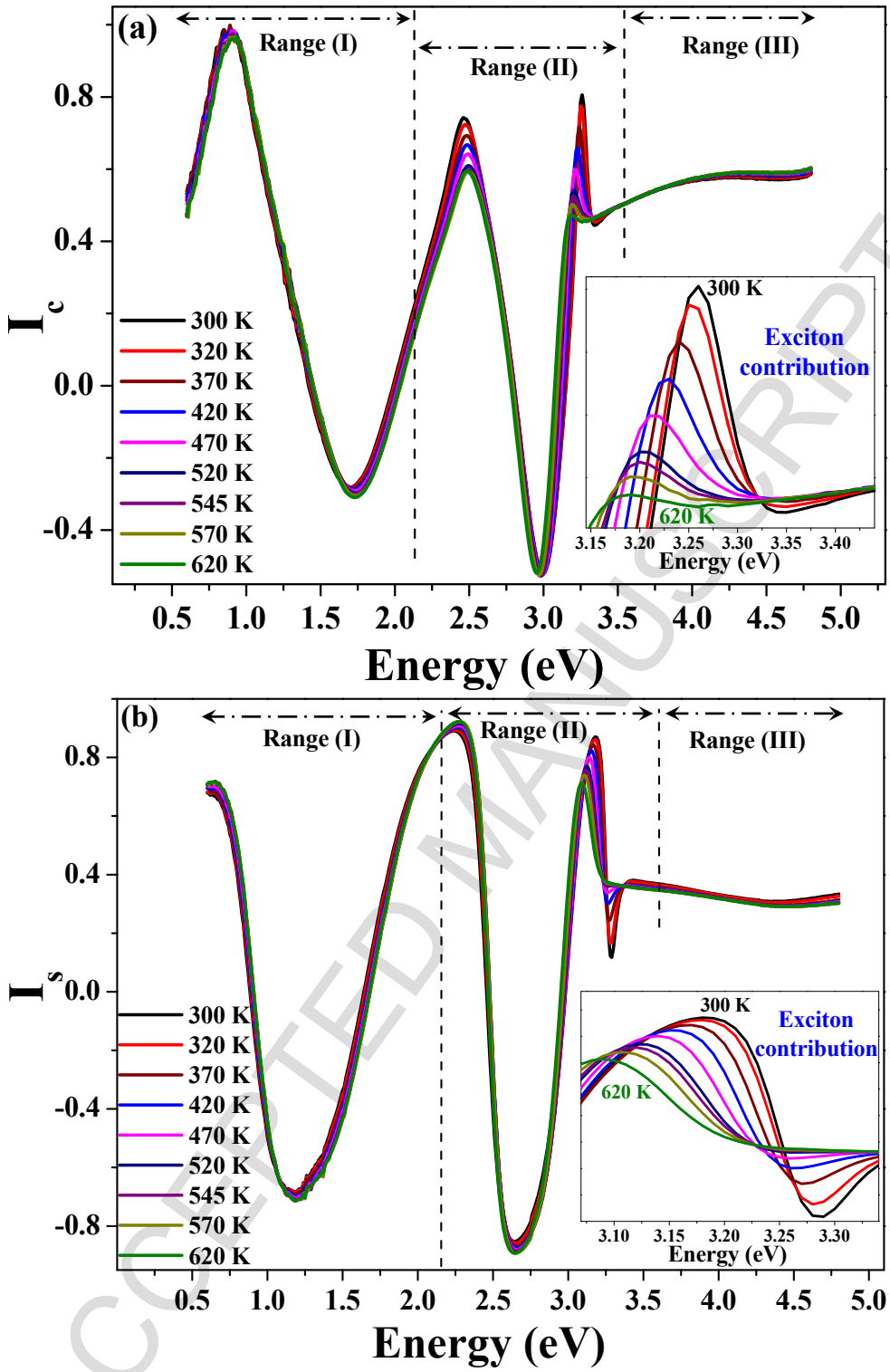

Fig. 1. Temperature dependence of ellipsometric experimental spectra (Ic, Is) of ZnO at an angle of incidence of 70°. The temperature varies from 300 K to 620 K.

3.1.1 Modeling of ellipsometric data by constrained cubic splines

A physical model is required to extract optical constants, thickness of different layers and their composition from the analysis of the Ic and Is spectra. Experimental SE spectra are fitted by minimizing the following mean-square error (χ^2) using the Levenberg-Marquardt [8]:

$$\chi^2 = \frac{1}{N}\sum_{i=1}^{N}\left(\frac{I_{C_{i(th)}} - I_{C_{i(exp)}}}{\delta I_C}\right)^2 + \left(\frac{I_{S_{i(th)}} - I_{S_{i(exp)}}}{\delta I_S}\right)^2, \qquad \text{Eq. (3)}$$

where $I_{C_{i(th)}}$, $I_{S_{i(th)}}$ and $I_{C_{i(exp)}}$, $I_{S_{i(exp)}}$ are the theoretical and experimental values of I_C and I_S, respectively. N is the number of collected data. δI_C and δI_S are the standard deviation of ellipsometry measurements.

In our previous work [11], different structural techniques have been used to study physical properties of ZnO/Si films elaborated with the similar sol-gel method reported in this paper. We have found that the ZnO film is composed of three ZnO porous sublayers on SiO_2/Si substrate. Thereby, the physical model used for SE data analysis is shown in Fig. 2. In this model each layer is considered as a mixture between ZnO and void described by an effective dielectric function according to the Bruggeman effective medium theory [28]. In the modeling, the known parameters are the dielectric functions of Si substrate [29] and SiO_2 [30]. Also, the unknown parameters are the thickness of each layer, the volume fractions and the dielectric function of ZnO.

The thickness and the composition of each layer are determined after optimization of the sample structure in the ZnO transparence range (I). The SiO_2 native oxide thin sublayer is set to 3 nm. The ZnO layer thickness and volume fraction values are given in Table 1.

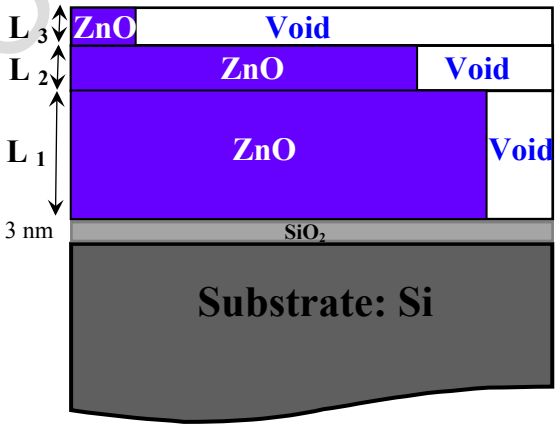

Fig. 2. Physical model of ZnO/Si sample.

Table 1. Composition and thickness of each sublayer associated to the model in Fig. 1.

Sublayer	**L_1**	**L_2**	**L_3**
Thickness (nm)	170	60	50
ZnO (%)	86	72	6
Void (%)	14	28	94

In the range (I), the period of oscillations depends on the film thickness. The expansion of the thickness between 300 K to 620 K can be calculated by the following equation:

$$\Delta L = \alpha_{\parallel c} L_0 (T - T_0), \qquad \text{Eq. (4)}$$

where $\alpha_{\parallel c}$ is the thermal expansion coefficient along the c-axis i.e the axis perpendicular to the substrate. T is the temperature and L_0 is the film thickness at T_0 = 300 K.

For $\alpha_{\parallel c}$, we choose the tabulated constant ($47\ 10^{-7}\ K^{-1}$) at 600 K [31]. According to the film thickness (280 nm) at 300 K, the highest variation of thickness ΔL is equal to 0.42 nm. As result, the ZnO thickness ($L=L_0+\Delta L\approx L_0$) is almost independent of temperature. Consequently, the optical path length is almost constant ($n_r L(T)\approx n_r L_0$) enabling the reproduction of the same oscillations with temperature as is seen in the energy range (I). Thus, the physical model (Fig. 2) is the same for all temperature ranging from 300 K to 620 K.

Once the physical model is determined, we use the CCS technique, which is more suitable for the determination of the dielectric function with temperature. The principle of CCS method is based on the determination of the imaginary part of dielectric function by a collection of connected splines. Each spline is given by third order polynomial that links successive energy nodes [12]. Note that a too high number of nodes may induce some correlation between them. Since the ZnO material exhibits an exciton effect around its band-gap (3.37 eV) [1], it is necessary to introduce more nodes around this band-gap but also around all particular spectral features shown in the Fig. 1. For this, the imaginary dielectric function of ZnO were divided into a set of splines using 20 nodes located at 0.6, 1, 2, 2.1, 2.3, 2.5, 2.9, 3, 3.1, 3.2, 3.3, 3.34, 3.36, 3.37, 3.38, 3.4, 4.0, 4.5, 5.0, 6.0 eV. The intrinsic ZnO is transparent in low energy spectral range. In the previous work [11], the transparent range for ZnO is until to 2 eV.

Hence, the imaginary part of dielectric function is set to zero from 0.6 eV to 2 eV and the 17 nodes between 2.1 and 6.0 eV were used in the data fitting. The fitted parameters are the spline ordinate components associated to the selected energy nodes and the dielectric constant at high energy ε_∞. Through these splines, the $I_{C_{i(th)}}$ and $I_{S_{i(th)}}$ are calculated and compared with experimental measurements $I_{C_{i(exp)}}$ and $I_{S_{i(exp)}}$ by minimizing the mean square error χ^2. The fit yielding the lowest residual χ^2 is kept as the solution. Good agreement between measured and calculated ellipsometric spectra (Ic, Is) at 300 K, 420 K, 520 K and 620 K is shown in Fig. 3. For spectra recorded at higher temperature, the nodes between 2.9 eV and 3.4 eV are shifted to lower energy. This shift reproduces the same temperature dependence of measured spectra as shown in Fig. 1. The real part is calculated from the Kramers-Kronig relations.

3.1.2 Dielectric function of ZnO

The corresponding real and imaginary parts of ZnO dielectric function are depicted in Fig. 4. The pick of the real part (see the insert in Fig. 4a) is shifted and its amplitude decreases with increasing temperature. Similarly, the absorption tail and the exciton band displayed in the insert in Fig. 4b are shifted to lower energy as the temperature increases. We attribute E_T to the intense electronic transition displayed in Fig. 4b. A typical exciton band of crystallized ZnO stills up to 420 K as shown in the top of the insert of Fig. 4b and in the Fig. 3. However, for the temperature higher than 420 K, the sharp of ZnO exciton band becomes widely flattening and blue-shifted. Even if the CCS method is adequately to evaluate the variation of the ZnO dielectric function with temperature, it is unable to give the physical parameters such as the band-gap energy or the exciton binding energy. For this reason, we have fitted by Tanguy model the ZnO dielectric function obtained by CCS method. The result is given in Fig. 5. Five free parameters is considered in the Tanguy dispersion: the amplitude factor (A), the band-gap energy (E_g), the exciton binding energy (R), the damping factor (Γ) and the dielectric constant at high photon energy (ε_∞) [11]. This dispersion takes into account the electronics transitions around the band-gap and the Wannier exciton effect of semiconductor material.

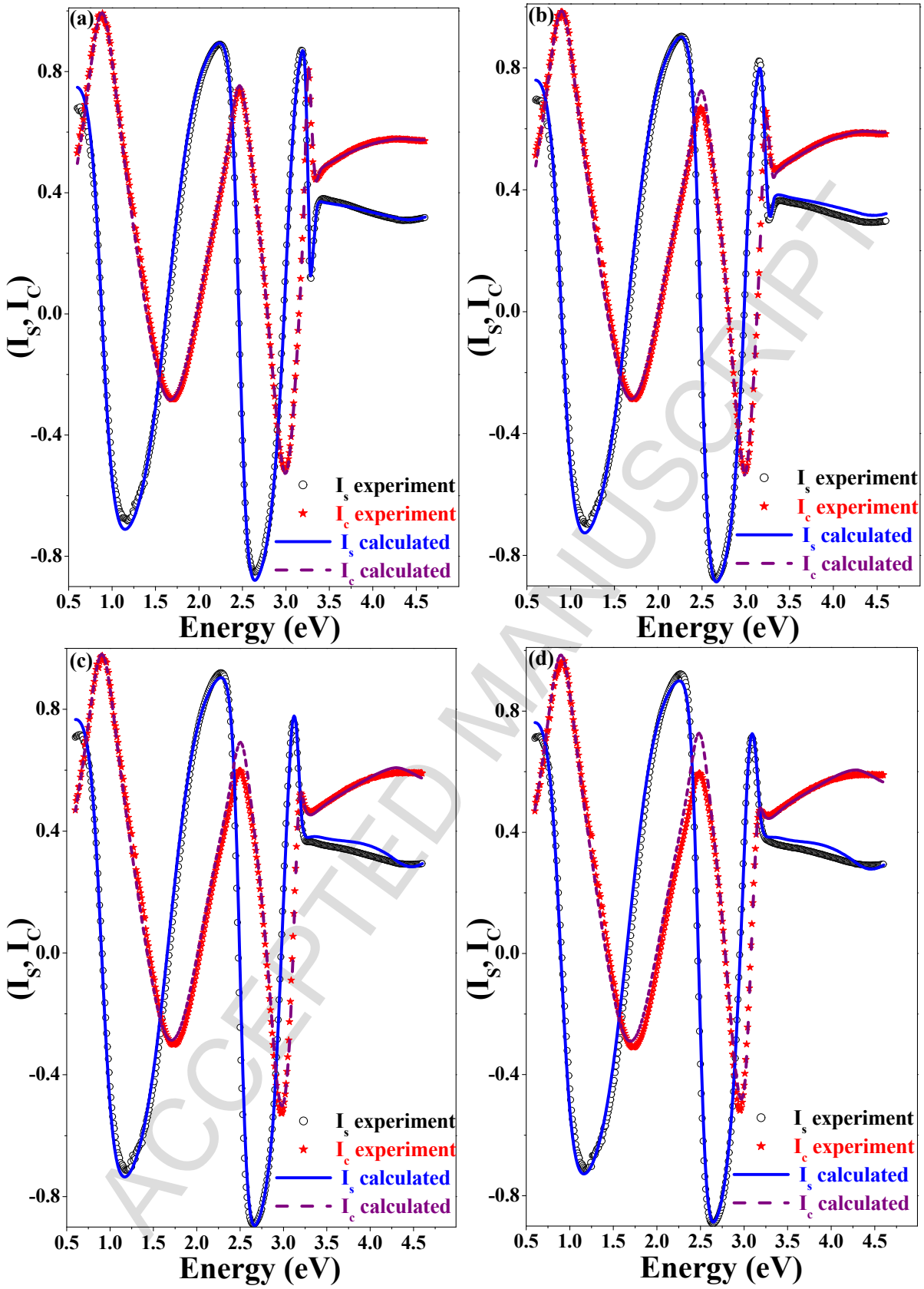

Fig. 3. Measured and calculated by CCS ellipsometric spectre (Ic, Is) of ZnO at (a) 300 K, (b) 420 K, (c) 545 K and (d) 620 K.

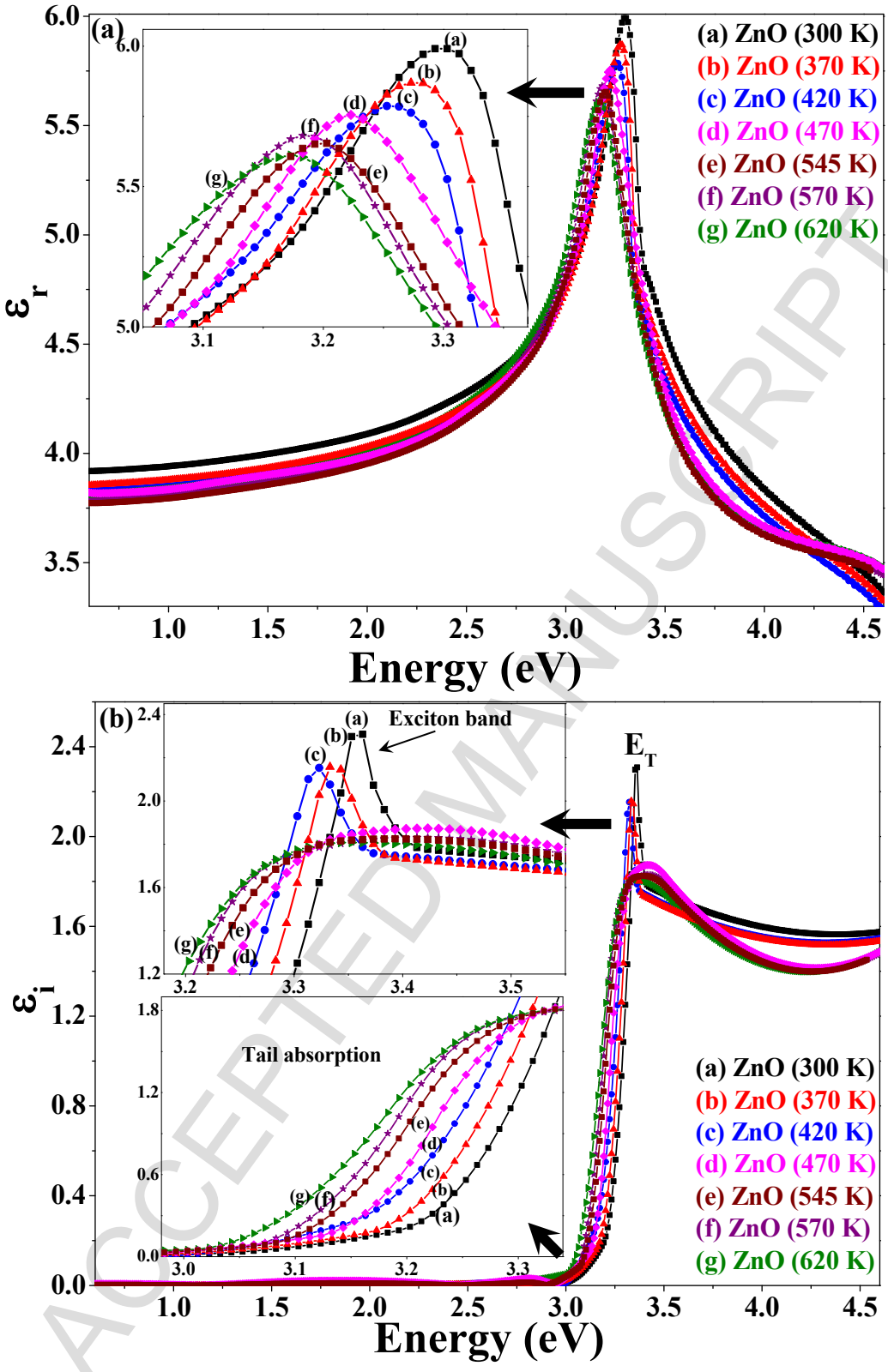

Fig. 4. (a) Real and (b) imaginary parts of ZnO dielectric function determined by CCS.

The Tanguy dispersion reproduces accurately the absorption tail and the exciton band of CCS dielectric function from 300 K to 420 K (see the insert in Fig. 5). However, for temperature higher than 470 K, a disagreement between Tanguy dispersion law and the CCS dielectric

function can be observed in this figure. Unlike the CCS dielectric function, Tanguy shows a narrow band exciton. This disagreement is also shown in Fig. 6a by the abruptly increasing of χ^2 from the temperature 470 K (Fig. 6a). For that, we have then fitted the CCS dielectric function by the TL model. The results are given in Fig. 5.

In addition of E_g, A and ε_∞, two other free parameters: the energy of the absorption around band edge (E_0) and the broadening parameter associated to the absorption band (C) are fitted to determine the dielectric function of ZnO [23]. This dispersion law combines the empirical Tauc's expression for the band edge onset with the absorption around band-gap energy given by the classical Lorentz oscillator. We note that the TL dispersion law with one oscillator (A, E_0, C) is unsuitable for reproduce the CCS dielectric function. Whereas, the TL dispersion with two oscillators is appropriate for reproducing the broadening of the absorption band in the temperature range of 470 K to 620 K as can be seen in the insert of Fig. 5. Nevertheless, in the temperature range of 300 K to 420 K, the TL model and the CCS show a disagreement concerning the broadness and the amplitude of the pick of dielectric function.

Furthermore, the smaller χ^2 values are obtained in the 300 K to 420 K and 470 K to 620 K temperature ranges for the Tangy and TL models, respectively. In addition, the temperature range 420 K to 470 K can be considered as the threshold temperature between Tanguy and TL dispersion laws. This threshold temperature can be explained by the exciton quenching. Fig. 6b shows the temperature dependence of the exciton binding energy (R) determined by the Tanguy dispersion. This figure also shows the kinetic energy in the ZnO film. We have found that its follows $(3/2)k_BT$ energy with the temperature (T). Note that k_B is the Boltzmann constant. Above the $(3/2)k_BT$, the R value is almost constant as can be seen in Fig. 6b. In this Fig, the R value crosses the kinetic energy line at around 430 K traducing the equilibrium between the Coulomb force of exciton and the kinetic energy in the film. Below the $(3/2)k_BT$ line, the exciton energy is quenched. This thermal energy at around 430 K allows the quenching of the exciton and subsequently the temperature range validity of TL dispersion law. Hence, the $(3/2)k_BT$ traduces that the exciton has three degree of freedom.

The temperature dependence of the E_T energy (extracted from Fig. 4) is shown in Fig. 7. Firstly, E_T values decrease up to the temperature 420 K. This E_T transition is assigned to the free exciton transition energy:

$$E_T = Eg–R. \qquad \text{Eq. (5)}$$

Then, the E_T is blue-shifted by 66 meV at the temperature 470 K. This energy value is in the same energy order as R (56 meV). Hence, this shift is due to the quenching of the exciton just below the conduction band allowing to the transition between the valence band to the conduction band. Finally, the E_T value at temperature higher than 470 K is attributed to the band-gap transition. In the insert of Fig. 7, it is shown the temperature dependence of the band-gap energy. Indeed, we assume that below 420 K, the band-gap energy value is incremented by the R energy (66 meV). Above 420 K, only the band-gap energy value is considered. This band gap energy is varying linearly in the studied temperature range in agreement with literature [33].

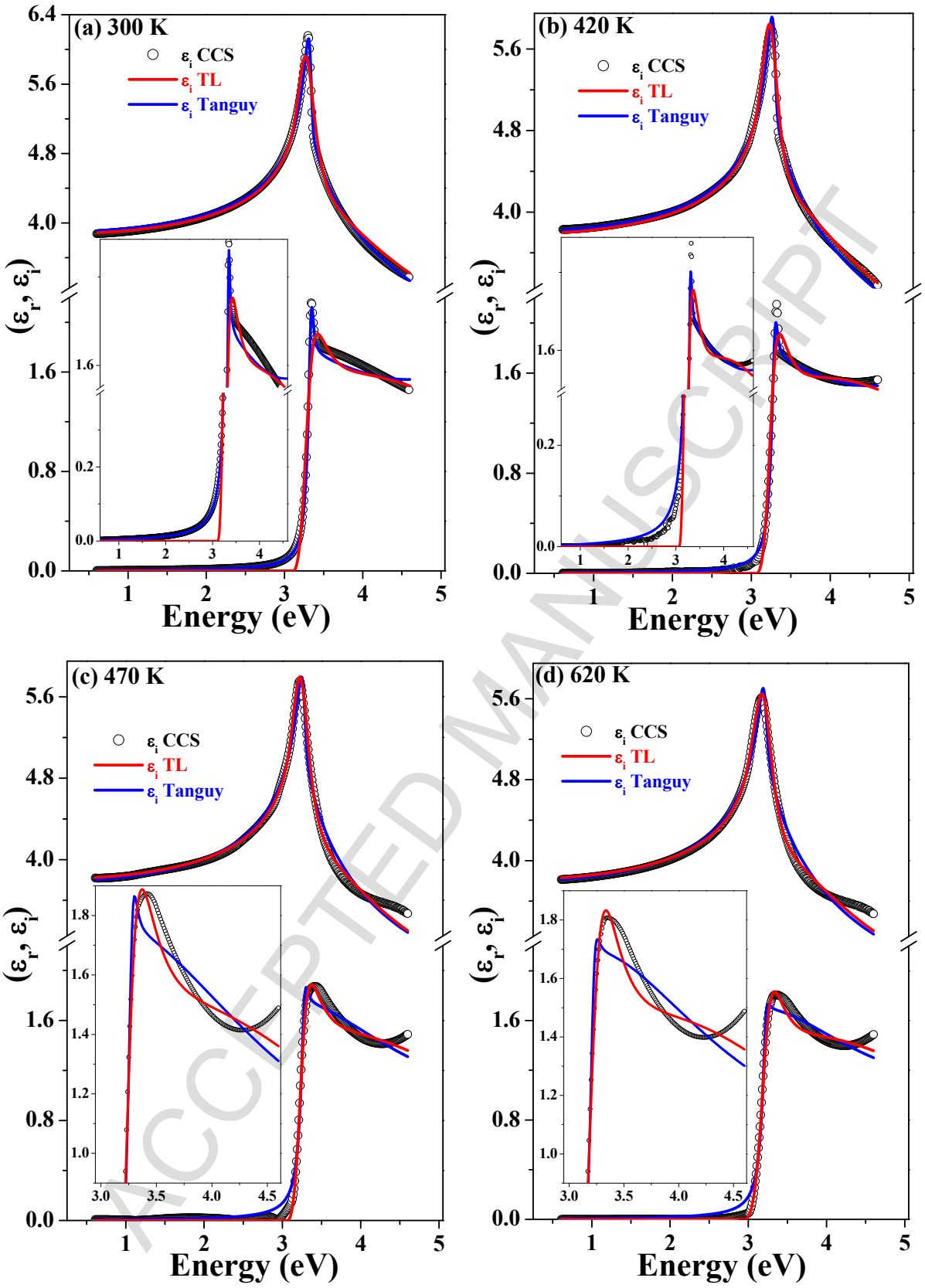

Fig. 5. Real and imaginary parts of dielectric function of ZnO by CCS fitted by TL and Tanguy dispersion laws at (a) 300 K, (b) 420 K, (c) 470 K and at (d) 620 K.

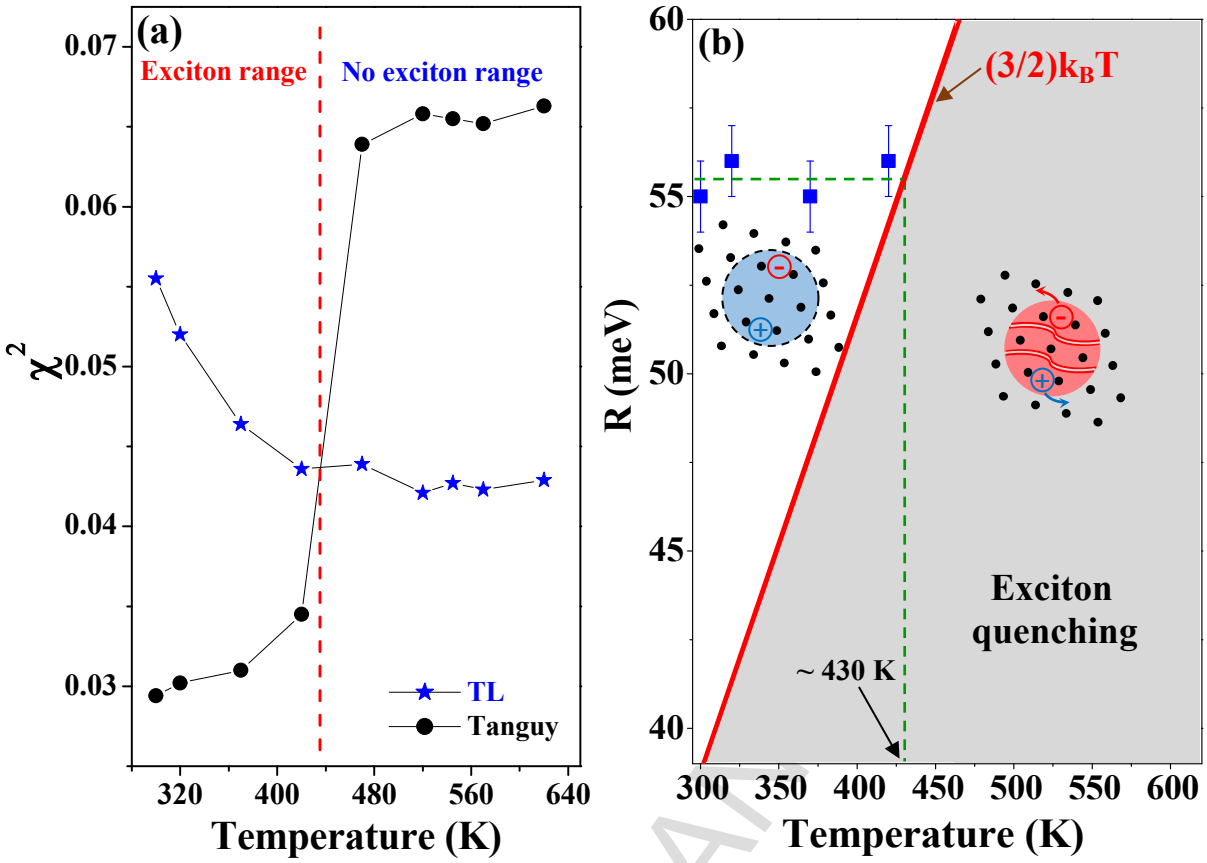

Fig. 6. Temperature dependence for (a) χ^2 and (b) R.

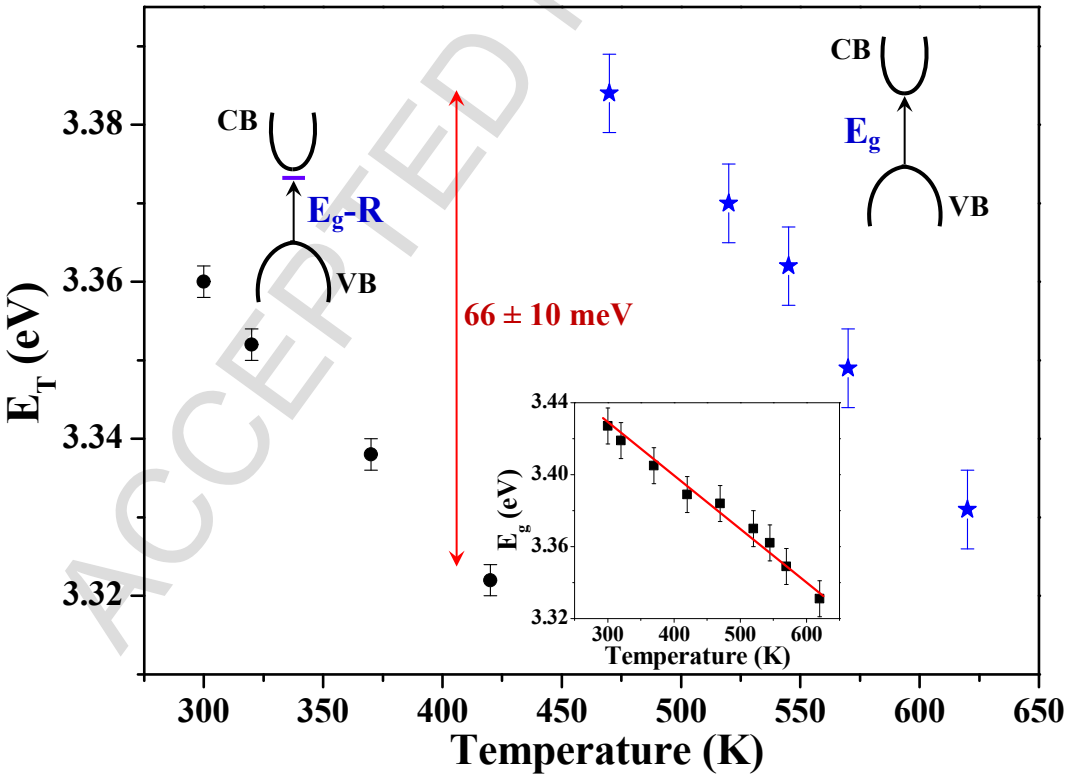

Fig. 7. Temperature dependence of electronic transition E_T extracted from imaginary dielectric function part in Fig. 4.

3.2 Spectroscopic Photoluminescence measurements

Fig. 8 depicts the ZnO luminescence spectra (log plot-normalized scale) in the UV range 2.85 eV–3.42 eV for temperatures comprised from 300 K to 620 K. The increase of temperature induces a red-shift for UV band with a decrease by 3 times in intensity. We note, also, than despite the decrease in intensity, the PL still up to the highest temperature reliable by our setup (620 K). Additionally, it is clear that the luminescence band is asymmetric up to 470 K. This band includes two shoulders at its extremity (1) and (3). Hence, we can distinguish three contributions marked (1), (2) and (3) in Fig. 8. Note that the energetic position of (2) band is nearly equidistant to the bands (1) and (3). Their energetic difference is around to (72 meV) the longitudinal optical phonon energy of ZnO [34]. Therefore, we propose to attribute the three peaks (1), (2) and (3) to FX and its first (FX') and second (FX'') replica phonons, respectively. The FX' intensity is higher than the FX one as it has been already observed [33, 35].

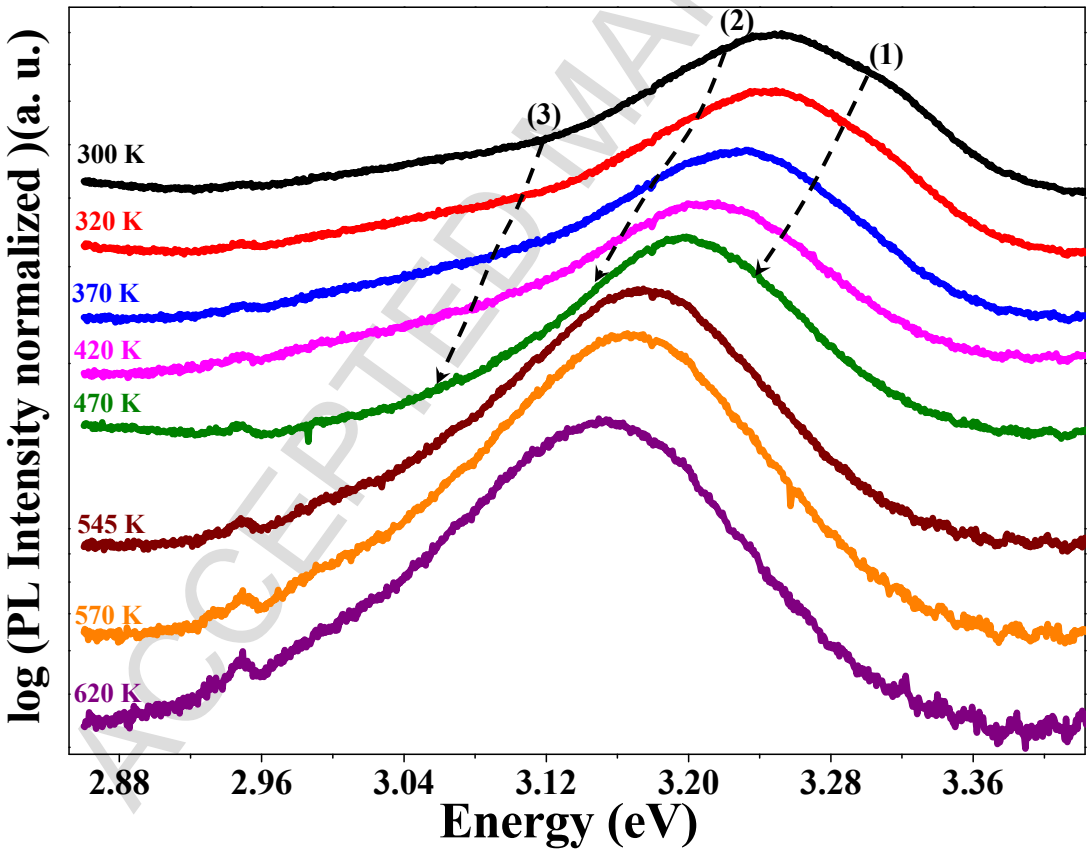

Fig. 8. Temperature dependence PL spectra of near-band-edge emissions of ZnO from 300 K to 620 K.

To get deeper insight of the PL exciton contributions occurring in ZnO thin films, we have carried out the PL measurement in the temperature range 10 K–280 K in a He closed-circuit cryostat. The luminescence spectrums from 10 K to 620 K are summarized in Fig. 9. First of all, defects in the low energy range are observed only in this second set of measurements revealing small difference with PL measurements above RT. This difference at low energy displays despite the relatively structure crystalline quality already reported [11]. We can clearly see that the UV band decreases in intensity with the temperature mainly in the temperature range 300 K to 470 K. The band centered at 3.37 eV at 10 K may be attributed to free exciton transition (FX) in good agreement with the literature [1, 36]. A large band (3.3 eV to 3.35 eV) labeled (II) merges at 10 K. The origin of this band is not clear. According to the literature, some bound excitons are located in this energy range. The two-electron satellite transitions are observed in the range 3.32 eV–3.34 eV [37-39]. The acceptor-bound excitons (AX) are located in the range 3.35 eV–3.36 eV [37]. The exciton bound to the structural defects (Y_line) commonly seen in some II-VI semiconductor as ZnSe and ZnTe [38]. This Y_line exciton bound is situated at 3.33 eV [38]. In addition, the FX' is reported at 3.3 eV [39]. In our case, the FX' is already observed at temperature higher than 300 K as shown in Fig. 8. Hence, we attribute this band (II) to a combination between FX' and both or one of the two bound excitons AX and Y_line. The broad band at 3.19 eV may be assigned to the exciton bounded to the donor-acceptor pairs defects (DAP) [40].

Fig. 10 displays the temperature dependence of FX transition energy (E_{FX}) extracted from 10 K to 470 K. In literature, some empirical formulas are used to simulate this red-shift such as Varshni [41], Cody [42], Vina [43]… However, no physical origin of the modification of E_{FX} transition is clearly given by these models. Indeed here, this recorded shift can be explained by the contribution of two phenomena: the lattice expansion and the electron-phonon interactions [44]. The contribution of the lattice expansion can be modulated by the following formula [41]:

$$\Delta E^{lat}(T) = -D\frac{dE_g}{dp}\int_0^T \alpha_V(T')dT', \qquad \text{Eq. (6)}$$

where D is the bulk modulus of ZnO [45], $\frac{dE_g}{dp}$ the pressure dependent band gap [46] and α_V the thermal expansion coefficient [31].

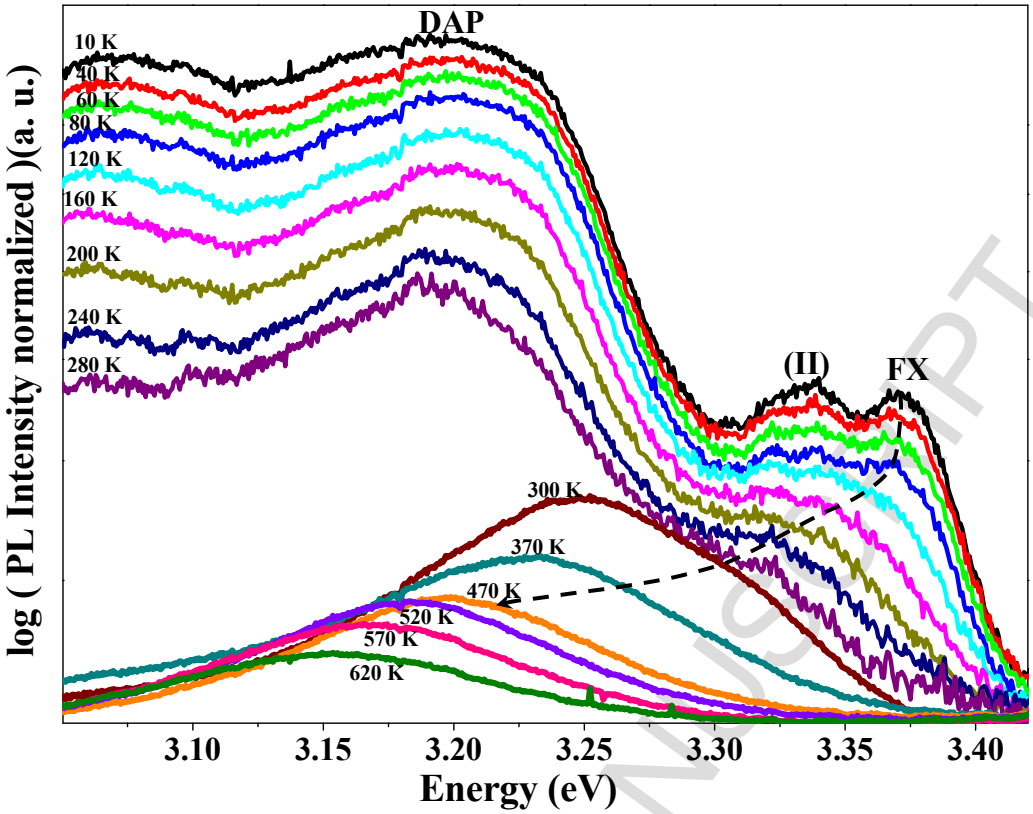

Fig. 9. Temperature dependence PL spectra of near-band-edge emissions of ZnO from 10 K to 620 K.

On the other hand, electron-phonon (e-pho) interaction leads to an additional shift for E_{FX} as describing by [47]:

$$\Delta E^{e-pho}(T) = -\frac{\alpha}{k_B}\int_0^{\infty}\frac{E\,\rho(E)}{e^{E/k_BT}-1}dE, \qquad \text{Eq. (7)}$$

α is free parameter which needs to be adjusted, E is the energy of phonon and ρ(E) is the normalized phonon density of states [48]. Hence, the total shift is the sum of these two contributions. The energetic position of FX is fitted using this equation:

$$E_{sim}(T) = E(0) + \Delta E^{lat}(T) + \Delta E^{e-pho}(T), \qquad \text{Eq. (8)}$$

where E(0) is the second parameter which needs to be adjusted.

The equation (8) reproduces the E_{FX} displacement from 10 K to 470 K in Fig. 10. The fitting parameters α and E(0) are 0.20 meV/K and 3.37 eV, respectively. The E_{FX} shifts to low energy by around 161 ± 8 meV in the temperature range 10 K–470 K. Hauschild *et al.*[17] are

measured, for thin ZnO film, almost the same displacement (165 meV) in the same temperature range for thin ZnO film. Hence, this result confirms our previous hypothesis of the localization of the E_{FX} in Fig. 8. The E^{e-pho} is closer to E_{FX} than E^{lat} as shown in Fig. 10. As consequence, the e-pho interactions have the major contribution in the red-shift of E_{FX} band with increasing temperature. The small contribution of the lattice expansion confirms the same constant physical model with temperature used in ellipsometry characterization. As shown in Fig. 8, the UV band is more symmetric at temperature higher than 470 K. We present the position of the half higher energetic E_{max} in Fig. 10. Using the fitting parameter of E_{sim}, we can extrapolate fitted result up to 620 K. We remark that E_{max} from 520 K to 620 K are located uppermost E_{sim}. This blue-shift can be the consequence of the recombination between hole in the valence band and electron in the conduction band. Although, this enhances to conclude the quenching of exciton around 470 K as in agreement with ellipsometry results.

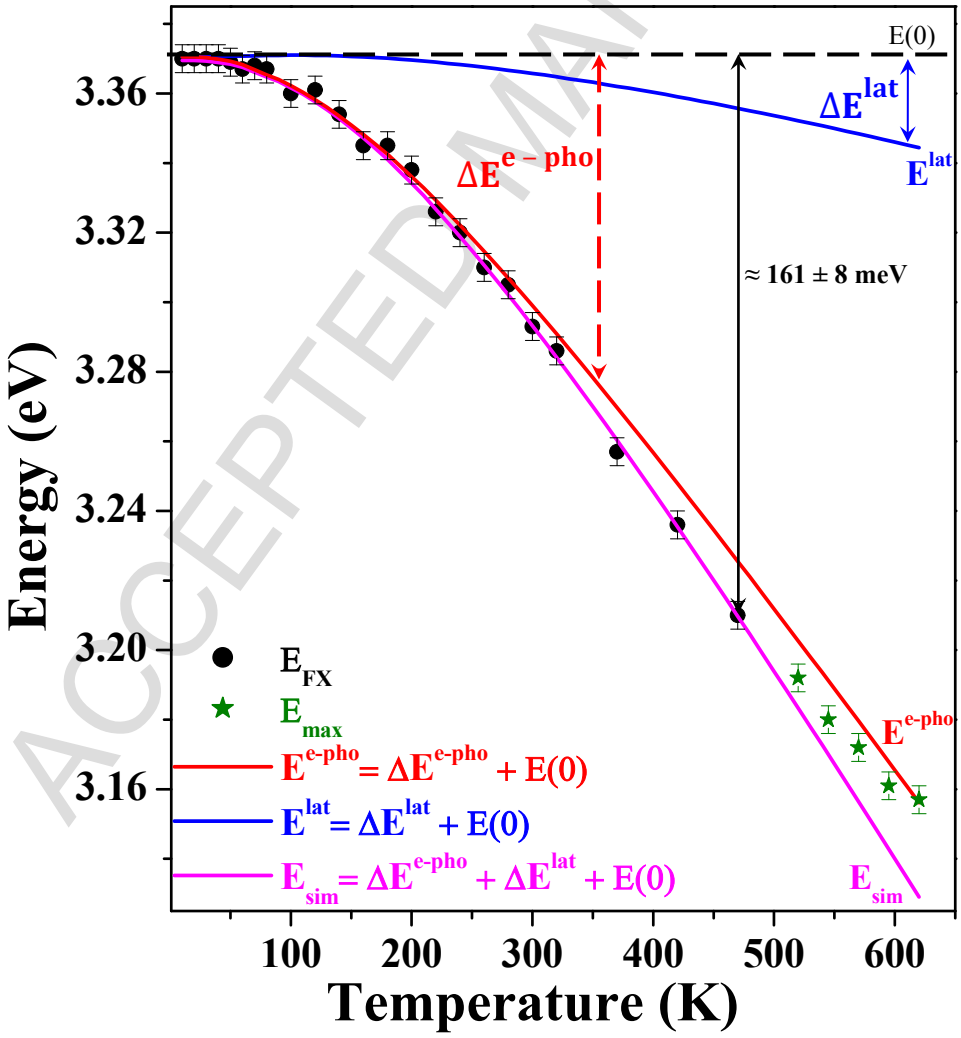

Fig. 10. Temperature dependence of the FX transition energy. Fitting models composed by two intrinsic contributions of ZnO: lattice expansion and electron-phonon interaction.

4. Conclusion

In summary, ZnO thin film synthesized by sol-gel method was subject of a detailed optical study by ellipsometry over the temperature range 300 K to 620 K and by PL in the temperature range of 10 K to 620 K. This study was highlighted the temperature dependent dielectric function, electronic transitions and exciton binding energy of ZnO thin film. We have demonstrated that the constrained cubic splines approximation is a suitable numerical method for determining the temperature dependence of the dielectric function of ZnO. The obtained dielectric function was also extracted by Tauc-Lorentz and Tanguy dispersion equations. Tanguy model was found to be more appropriate for optical responses of ZnO thin film in the temperature range of 300 K to 420 K. However, the Tauc-Lorentz reproduces correctly the ZnO dielectric function in 470 K to 620 K temperature range. We found that the ZnO exciton band is widely flattening and blue-shifted by the same energy order than the exciton binding at 470 K. In 420 K to ~ 520 K temperature range, both SE and PL techniques show that the exciton is quenched. These results infer that the quenching of exciton is occurred when the equilibrium between the Coulomb force of exciton and its kinetic energy in ZnO film is reached. This kinetic energy was found to induce a three degree of freedom of exciton.

Acknowledgment

The authors would like to acknowledge Pascal Franchetti (LCP-A2MC) for technical assistance in PL measurements.

References

[1] Ü. Özgür, Y. I. Alivov, C. Liu, A. Teke, M. A. Reshchikov, S. Doğan, V. Avrutin, S.J. Cho, H. Morkoç, Journal of Applied Physics 98, (2005) 041301.

[2] S. Sharma, S. Vyas, C. Periasamy, P. Chakrabarti, Superlattices and Microstructures 75 (2014) 378–389.

[3] K. N. Abbas, N. Bidin, Applied Surface Science 394 (2017) 498–508.

[4] R. Joaniso, O.K. Tan, Semiconductor Gas Sensors, Woodhead Publishing, Cambridge, 2013.

[5] M. Norek, G. Łuka, M. Włodarski, Applied Surface Science 384 (2016) 18–26.

[6] S. Sharma, C. Periasamy, Superlattices and Microstructures 73 (2014) 12–21.

[7] R.M.A. Azzam, N.M. Bashara, Ellipsometry and Polarized Light, North-Holland, Amsterdam, 1977.

[8] H. Fujiwara, Spectroscopic Ellipsometry: Principles and Applications, Wiley, Japan, 2007.

[9] C. Besleaga, G.E. Stan, A.C. Galca, L. Ion, S. Antohe, Applied Surface Science 258 (2012) 8819–8824.

[10] D. Pal, J. Singhal, A. Mathur, A. Singh, Su. Dutta, S. Zollner, S. Chattopadhyay, Applied surface science 421 (2016) 341–348.

[11] M.-B. Bouzourâa, Y. Battie, S. Dalmasso, M.-A. Zaïbi, M. Oueslati, A. En Naciri, Superlattices and Microstructures, 104 (2017) 24–36.

[12] M. Gilliot, A. Hadjadj, M. Stchakovsky, Applied Surface Science 421 (2017) 453–459.

[13] B. Johs, J.S. Hale, Phys. Status Solidi (a) 205 (2008) 715–719.

[14] M. Dressel, G. Grüner, Electrodynamics of Solids, Optical Properties of Electrons in Materials, Press Cambridge, Cambridge University, 2002.

[15] R. C. Rai. Journal of Applied Physics 113 (2013) 153508.

[16] R. C. Rai, M. Guminiak, S. Wilser, B. Cai, M. L. Nakarmi, Journal of Applied Physics 111 (2012) 073511.

[17] R. Hauschild, H. Priller, M. Decker, J. Brückner, H. Kalt, C. Klingshirn, physica status solidi 3 (2006) 976–979.

[18] Y.C. Liu, J.H. Hsieh, S.K. Tung, Thin Solid Films 510 (2006) 32–38.

[19] S. Logothetidis, A. Laskarakis, S. Kassavetis, S. Lousinian, C. Gravalidis, G. Kiriakidis, Thin Solid Films 516 (2008) 1345–1349.

[20] M. Gilliot, C. Eypert, A. Hadjadj, Journal of Applied Physics 114 (2013) 183513.

[21] J.M. Khoshman, J.N. Hilfiker, N. Tabet, M.E. Kordesch, Applied Surface Science 307 (2014) 558–565.

[22] Á. Németh, C. Major, M. Fried, Z. Lábadi, I. Bársony, Thin Solid Films 516 (2008) 7016–7020.

[23] G.E. Jellison, F.A. Modine, Appl. Phys. Lett. 69 (1996) 371–373.

[24] L. Znaidi, Materials Science and Engineering B 174 (2010) 18–30.

[25] Y.-S. Kim, W.-P. Tai, S.-J. Shu, Thin Solid Films 491 (2005) 153–160.

[26] A.-S. Keita, A. En Naciri, F. Delachat, M. Carrada, G. Ferblantier, A. Slaoui, Journal of Applied Physics 107 (2010) 093516.

[28] M.-B. Bouzourâa, A. En Naciri, A. Moadhen, H. Rinnert, M. Guendouz, Y. Battie, A. Chaillou, M.-A. Zaïbi, M. Oueslati, Materials Chemistry and Physics 175 (2016) 233–240.

[28] R.J. Gehr, R.W. Boyd, Chemistry of Materials 8 (1996) 1807–1819.

[29] E.D. Palik, Handbook of Optical Constants of Solids, Elsevier, London, 1997.

[30] A. En Naciri, P. Miska, A.-S. Keita, Y. Battie, H. Rinnert, M. Vergnat, Journal of Nanoparticle Research 15 (2013) 1538.

[31] H. Ibach, physica status solidi 33 (1969) 257–265.

[32] C. F. Klingshirn, B. K. Meyer, A. Waag, A. Hoffmann, J. Geurts, From fundamental Properties Towards Novel Applications, Springer, New York, 2010.

[33] M. S. Ramachandra Rao, T. Okada, ZnO Nanocrystals and Allied Materials, Springer, India, 2014.

[34] R. Liu, A. Pan, H. Fan, F. Wang, Z. Shen, G. Yang, S. Xie, B. Zou, Journal of physics: Condensed Matter 19 (2007) 136206.

[35] D. W. Hamby, D. A. Lucca, M. J. Klopfstein, G. Cantwell, Journal of Applied Physics 93 (2003) 3214.

[36] G. Nam, H. Park, H. Yoon, J. S. Kim, J.-Y. Leem, Current Applied Physics 13 (2013) S168–S171.

[37] A. Teke, Ü. Özgür, S. Doğan, X. Gu, Hadis Morkoç, B. Nemeth, J. Nause, H. O. Everitt, Physical Review B 70 (2004) 195207.

[38] B. K. Meyer, 1, H. Alves, D. M. Hofmann1, W. Kriegseis, D. Forster, F. Bertram, J. Christen, A. Hoffmann, M. Straßburg, M. Dworzak, U. Haboeck, A. V. Rodina, physica status solidi 241 (2004) 231–260.

[39] F. Jiang, J. Dai, L. Wang, W. Fang, Y. Pu, Q. Wang, Z. Tang, Journal of Luminescence 122–123 (2007) 162–164.

[40] B. Wu, Y. Zhang, Z. Shi, X. Li a, X. Cui, S. Zhuang, B. Zhang, G. Du, Journal of Luminescence 154 (2014) 587–592.

[41] Y.P. Varshni, Physica 34 (1967) 149–154.

[42] G.D. Cody, Hydrogenated Amorphous Silicon, Semiconductors and Semimetals Part b, Pankove, New York, 1984.

[43] A. Mabrouk, N. Lorrain, M. L. Haji, M. Oueslati, Superlattices and Microstructure 77 (2015) 219–231.

[44] D. Lüerßen, R. Bleher, H. Kalt, Physical Review B 61 (2000) 15812–15816.

[44] J. Serrano, A. Romero, F. Manjón, R. Lauck, M. Cardona, A. Rubio, Physical Review B 69 (2004) 094306.

[46] A. Mang, K. Reimann, S. Rübenacke, Solid State Communications 94 (1995) 251–327.

[47] R. Pässler, Journal of Applied Physics 89 (2001) 6235–6240.

[48] J. Serrano, F. Manjón, A. Romero, F. Widulle, R. Lauck, and M. Cardona, Physical Review Letters 90 (2003) 055510.

Highlights

- Constrained cubic splines approximation was demonstrated as a suitable numerical method for determining the temperature dependence of the dielectric function of ZnO.
- Tanguy optical model can be consider as the more appropriate dispersion model for determining the optical responses of ZnO thin film in the temperature range of 300 K to 420 K.
- Tauc-Lorentz optical model can be consider as the more appropriate dispersion model for determining the optical responses of ZnO thin film in the temperature range of 470 K to 620 K.
- Both ellipsometry and photoluminescence techniques show the quenching exciton in 420 K to ~ 520 K temperature range.
- The exciton quenching was attributed to the equilibrium between the Coulomb force of exciton and its kinetic energy in ZnO film.